

# Corrosion Inhibition of Aluminium by *Alchemilla vulgaris* L. Extract in 3 % NaCl Solution

 Ivana Martinović,\*  Zora Pilić,  Gloria Zlatić, Marija Barišić, Stipe Čelan

Department of Chemistry, Faculty of Science and Education, University of Mostar, Matice hrvatske bb, Mostar, Bosnia and Herzegovina

\* Corresponding author's e-mail address: ivana.martinovic@fpmoz.sum.ba

RECEIVED: December 3, 2021 \* REVISED: January 17, 2022 \* ACCEPTED: January 18, 2022

**Abstract:** Extract of *Alchemilla vulgaris* L. was investigated as eco-friendly corrosion inhibitor for aluminium in 3 % NaCl using electrochemical techniques. According to the results, inhibition efficiency increases with the increase concentration of extract and the highest efficiency (~80 %) is recorded for the maximal concentration of extract (1.0 g L<sup>-1</sup>). The inhibition activity of extract occurs by the spontaneous physisorption ( $\Delta G \approx -16$  kJ mol<sup>-1</sup>) on active sites of aluminium surface that follows Freundlich isotherm. Polarization curves showed that *Alchemilla vulgaris* L. extract acts as a mixed-type inhibitor. The effect of temperature on the aluminium corrosion and inhibition action of extract was studied and the result showed that the corrosion rate increased and the inhibitor efficiency decreased with increase of temperature. The calculated values of the activation energy confirmed presence of inhibitive *Alchemilla vulgaris* L. extract on aluminium surface.

**Keywords:** aluminium, corrosion inhibition, *Alchemilla vulgaris* L. extract, adsorption, electrochemical methods.

## INTRODUCTION

ALUMINIUM and its alloys are one of the most attractive materials for a broad range of uses such as fabrication of cars and marine parts, pipes, construction and aircraft due their low density, high corrosion resistance and high mechanical strength.<sup>[1–3]</sup> High corrosion resistance of aluminium is due the spontaneous formation of a thin oxide film which separates the bare metal from the corrosive environment.<sup>[1–3]</sup> In the contact with acid, alkaline or media with aggressive anions (like Cl<sup>-</sup>), the protective oxide layer can be destroyed and metal may suffer serious corrosion.<sup>[2]</sup> An efficient method for metal protection is the use of inhibitors. The conventional organic and inorganic corrosion inhibitors have good corrosion inhibition efficiency but also have limited solubility and toxic properties. However, as a result of the increasing awareness of ecological and health risks caused by commercial inhibitors, there is a need to explore eco-friendly and highly efficient corrosion inhibitors. Natural products, such as aromatic and medicinal plants, have been used as naturally occurring corrosion inhibitors that are environment friendly, easily biodegradable, inexpensive and readily available.<sup>[1,3–8]</sup> Protection efficiency of plant

extract is attributed mainly to the presence of active compounds, such as phenols, flavonoids, tannins, terpenes, etc., which are known for their antimicrobial, antioxidant and anticorrosion activities. These compounds adsorb on active metal surfaces and form a protective layer that reduces the corrosion attack. Many natural products such as *Treulia africana* leaves,<sup>[1]</sup> *Linum usitatissimum* seeds,<sup>[7]</sup> rice straw extract,<sup>[8]</sup> *Polygonatum odoratum* extract<sup>[9]</sup> were investigated as green inhibitors for aluminium corrosion. It was found that these molecules adsorb spontaneously on aluminium surface mainly by physical adsorption and inhibition efficiency varied from 70 to 90 %.

In the present study, the corrosion inhibition of aluminium and adsorption properties of *Alchemilla vulgaris* L. extract in 3 % NaCl solution were investigated using electrochemical techniques. *Alchemilla vulgaris* L., a plant of Balkans region origin was chosen as a potential eco-friendly corrosion inhibitor for aluminium. *Alchemilla vulgaris* L. is used in traditional medicine, mainly for woman related diseases and has antioxidant, enzyme inhibitory and anticancer activity due its phenolic profile, rich in catechin, quercetin and its hexoside, luteolin, apigenin, gallic and caffeic acids.<sup>[10]</sup> The extract of *Alchemilla vulgaris* L. has previously been studied for its corrosion inhibiting

properties on copper in 1 M HCl<sup>[11]</sup> however there is no literature data on its inhibitory properties on other metals. *Alchemilla vulgaris* L. extract has complex chemical composition and corrosion inhibitory effect is due the presence of flavonoids, phenols, tannins, terpenes, carboxylic acids and essential oil.<sup>[10,11]</sup>

## EXPERIMENTAL PROCEDURE

The electrochemical measurements were performed at room temperature (25 °C) in a standard three electrode cell. Aluminium (99.99 %) was used as working electrode with the surface area exposed to the electrolyte 0.636 cm<sup>2</sup>. Prior to each measurement electrode was abraded by 1200 grade emery paper, degreased with ethanol in an ultrasonic bath, rinsed with ultra pure water (18.2 MΩ cm, produced by Millipore Simplicity UV Water Purification System) and polarized at -1.60 V vs. Ag | AgCl | 3 M KCl electrode for 30 seconds to remove airformed surface oxide.

For all measurements as a main electrolyte was used 3 % NaCl solution. The solution was prepared by dissolving of analytical grade purity NaCl salt in ultra pure water. The extract of *Alchemilla vulgaris* L. was tested as potential corrosion inhibitor of Al. The aerial parts of the *Alchemilla vulgaris* L. were collected during summer 2019, in Goranci, Mostar BiH and the plant material was dried in air for two weeks. A stock solution of extract (1.0 g L<sup>-1</sup>) was prepared after 3 h maceration in 3 % NaCl at a room temperature. Extract solutions (0.05, 0.10, 0.50 and 1.00 g L<sup>-1</sup>) were prepared by dilution of stock solution.

Corrosion behaviour of aluminium and inhibition efficiency of *Alchemilla vulgaris* L. extract was investigated by potentiodynamic polarization (PP), electrochemical impedance spectroscopy measurements (EIS) and cyclic voltammetry (CV). All measurements were performed with an Autolab PGSTAT320N controlled by a personal computer using Nova 1.5 software. Potentiodynamic polarization and impedance measurements were carried out after establishing a steady state open circuit potential. The potentiodynamic polarization curves were obtained in the potential ranges of -200 to 200 mV with respect to open circuit potential at a scan rate of 1.0 mV s<sup>-1</sup>. The corrosion current density ( $j_{corr}$ ) and corrosion potential ( $E_{corr}$ ) were obtained by extending the linear portion of the Tafel plots (both cathodic and anodic). Electrochemical impedance spectroscopy measurements were carried out at the open circuit potential ( $E_{OCP}$ ) using ±10 mV AC perturbation (rms) in the frequency range of 10 kHz to 5 mHz after a stationary state was achieved. The CV measurements were carried out in the potential range between -1.60 V and -0.70 V, with a scan rate of 30 mV s<sup>-1</sup>. Experiments were repeated three times to ensure the reproducibility.

## RESULTS AND DISCUSSION

### Potentiodynamic Polarization

The potentiodynamic polarization measurements were performed for the aluminium corrosion in 3 % NaCl solution with and without presence of AV extract and shown in Figure 1. It can be seen that polarization curves show a similar trend, but addition of AV extract reduces the corrosion current density indicating adsorption of extract on aluminium surface. The kinetic parameters, such as corrosion potentials ( $E_{corr}$ ), corrosion current densities ( $j_{corr}$ ) and Tafel slopes ( $\beta_a$ ,  $\beta_c$ ) were obtained from polarization curves and listed in Table 1. The surface coverage,  $\theta$  and inhibition efficiency,  $\eta$  were derived using the equations (1) and (2) and their values are also given in Table 1.

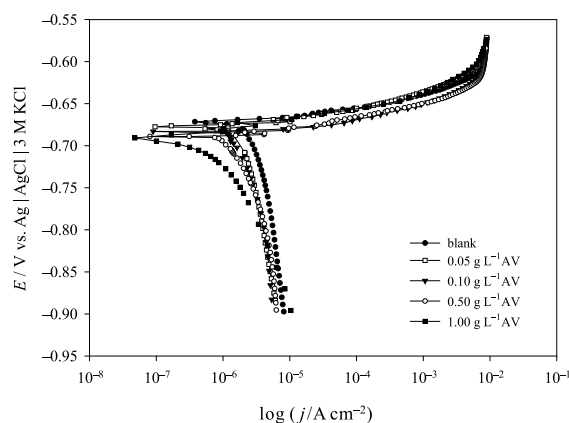
$$\theta = \frac{j_{corr}^0 - j_{corr}}{j_{corr}^0} \quad (1)$$

$$\eta = \theta \cdot 100 \quad (2)$$

where  $j_{corr}^0$  and  $j_{corr}$  represent the corrosion current densities of the Al electrode in absence and presence of the AV extract, respectively.

At all AV extract concentrations, the values of corrosion current density were reduced, compared with the value of blank solution. As the concentration of AV extract increases, the corrosion current density decreases (from 1.75 (blank) to 0.41  $\mu\text{A cm}^{-2}$  (1.0 g L<sup>-1</sup> AV extract)), and the inhibition efficiency increases (77 % for 1.0 g L<sup>-1</sup> AV extract) which indicates formation of a film of the extract on the Al surface.

According to the Table 1., the addition of AV extracts caused only small changes in the  $E_{corr}$  value (up to 20 mV) as compared to the blank hence it can be classified as mixed

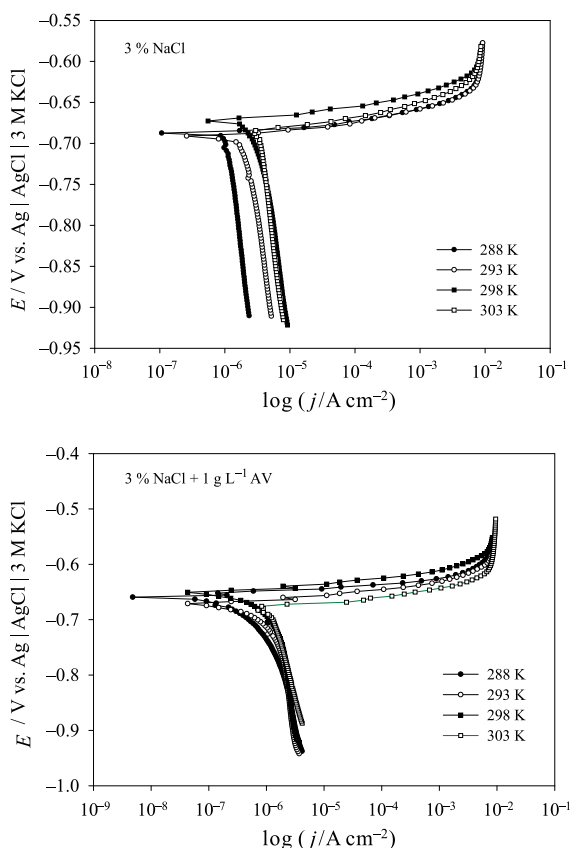


**Figure 1.** Potentiodynamic polarization curves for the Al electrode in 3 % NaCl solution, containing different concentrations of the AV extract (shown in figure);  $v = 1 \text{ mV s}^{-1}$ .

**Table 1.** Kinetic parameters from polarization measurements and calculated values of surface coverage,  $\theta$  and inhibition efficiency,  $\eta$  for the Al corrosion with and without presence of AV extract in 3 % NaCl.

Solution $\nu$ / g L <sup>-1</sup>	$E_{\text{corr}}$ / V	$j_{\text{corr}}$ / A cm <sup>-2</sup>	$\beta_a$ / mV dec <sup>-1</sup>	$\beta_c$ / mV dec <sup>-1</sup>	$\theta$	$\eta$ / %
Blank	-0.672	$1.75 \cdot 10^{-6}$	8.5	132.2	–	–
0.05	-0.693	$1.42 \cdot 10^{-6}$	10.5	114.4	0.188	18.8
0.10	-0.680	$1.24 \cdot 10^{-6}$	9.0	108.3	0.291	29.1
0.50	-0.682	$8.05 \cdot 10^{-7}$	11.0	100.4	0.540	54.0
1.00	-0.692	$4.06 \cdot 10^{-7}$	10.1	103.2	0.768	76.8

corrosion inhibitor. When the change in the  $E_{\text{corr}}$  value is greater than 85 mV, an inhibitor can be classified as anodic or cathodic.<sup>[4,8,12,13]</sup> Also, there is no significant variation in the values of cathodic and anodic Tafel slope with the addition of AV extract which indicates that the dissolution mechanism is not affected by the presence of extract and the inhibitor is working by blocking the active sites located on the surface of metal.<sup>[8,14]</sup>

**Figure 2.** Effect of temperature on polarization curves of Al corrosion rate in 3 % NaCl solution without and with 1.0 g L<sup>-1</sup> AV extract.

### Effect of Temperature

The effect of temperature on the corrosion of aluminium in 3 % NaCl in the absence and presence of 1.0 g L<sup>-1</sup> AV extract was investigated in the temperature range 15–30 °C by potentiodynamic polarization (Figure 2.). Kinetic parameters from potentiodynamic polarization curves are listed in Table 2.

From the Table 2., it is obvious that the corrosion current density increases with rise in temperature in both blank and AV extract samples. The decrease in the inhibition efficiency with a higher temperature (from 87 % at 288 K to 70.2 % at 303 K) is due an increased desorption rate that at higher temperature overcomes an adsorption rate.<sup>[6,15–17]</sup>

To determine the activation energy,  $E_a$  of aluminium corrosion with and without presence of 1.0 g L<sup>-1</sup> AV extract in 3 % NaCl the Arrhenius equation was used:

$$j_{\text{corr}} = A \exp\left(\frac{-E_a}{RT}\right) \quad (3)$$

where  $A$  is the Arrhenius pre-exponential factor,  $T$  the absolute temperature,  $E_a$  the activation energy for the corrosion process and the  $R$  is universal gas constant.

The activation energy was calculated from the slope of the Arrhenius plot ( $\ln(j_{\text{corr}})$  vs.  $1/T$ ) shown in Figure 3. The calculated  $E_a$  values for Al corrosion without and with presence of 1.0 g L<sup>-1</sup> AV extract are 52.7 and 89.2 kJ mol<sup>-1</sup>, respectively. The higher value of  $E_a$  in the presence of the AV extract may be due adsorbed inhibitive AV extract layer that acts as a physical barrier to charge and mass transfer.<sup>[6,8,18]</sup>

### Electrochemical Impedance Spectroscopy

To examine the inhibition activity of *Alchemilla vulgaris* L. extract on aluminium corrosion in 3 % NaCl, the impedance measurements were performed at the open circuit potential. Impedance spectra are presented in Figure 4. as Nyquist and Bode plots and interpreted by means of electrical equivalent circuits (EEC) shown in detail in Figure 4. In these

**Table 2.** Temperature effect on values of corrosion current density, corrosion potential, surface coverage and corrosion inhibition efficiency for the Al corrosion with and without presence of 1.0 g L<sup>-1</sup> AV extract in 3 % NaCl obtained from potentiodynamic polarization measurements.

$T / ^\circ\text{C}$	$\gamma / \text{g L}^{-1}$	$E_{\text{corr}} / \text{V}$	$j_{\text{corr}} / \text{Acm}^{-2}$	$\theta$	$\eta / \%$
15	blank	-0.685	$8.16 \cdot 10^{-7}$	–	–
	1.0	-0.662	$1.07 \cdot 10^{-7}$	0.869	86.9
20	blank	-0.691	$1.37 \cdot 10^{-6}$	–	–
	1.0	-0.671	$1.77 \cdot 10^{-7}$	0.871	87.1
25	blank	-0.672	$1.75 \cdot 10^{-6}$	–	–
	1.0	-0.659	$4.06 \cdot 10^{-7}$	0.768	76.8
30	blank	-0.683	$2.52 \cdot 10^{-6}$	–	–
	1.0	-0.670	$7.51 \cdot 10^{-7}$	0.702	70.2

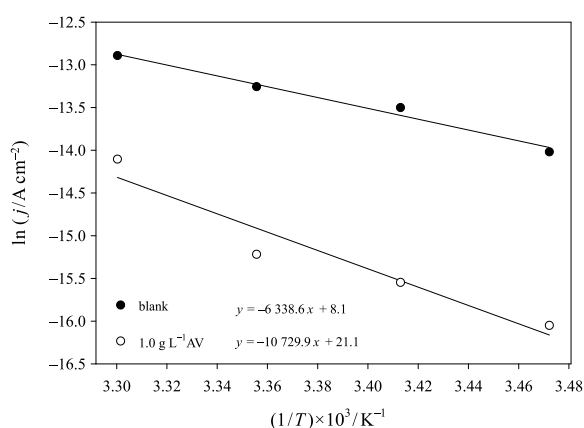


**Figure 3.** Arrhenius plots of Al in 3 % NaCl with and without 1.0 g L<sup>-1</sup> of AV extract.

circuits a constant phase element (CPE) was used and its impedance may be defined:

$$Z_{\text{CPE}}(\omega) = [Q(j\omega)^n]^{-1},$$

where  $Q$  is the constant,  $\omega$  is the angular frequency and  $n$  is the CPE power with values between 0.5 and 1. When  $n = 1$ , the CPE describes an ideal capacitor with  $Q$  equal to the capacitance ( $C$ ). For  $0.5 < n < 1$ , the CPE describes a distribution of dielectric relaxation times in frequency space, and when  $n = 0.5$  the CPE represents a Warburg impedance.

Selected EEC for describing impedance spectra of Al electrode in 3 % NaCl, without and with presence of AV extract (0.1 and 0.5 g L<sup>-1</sup>) consist of ohmic resistance,  $R_\Omega$  ( $\sim 5 \Omega \cdot \text{cm}^2$ ) in a serial connection with two time constants. The first time constant, at medium frequencies, is the result of the fast charge transfer process during the Al dissolution: the CPE<sub>1</sub> with power  $n$  close to 1.0 describes a capacitor

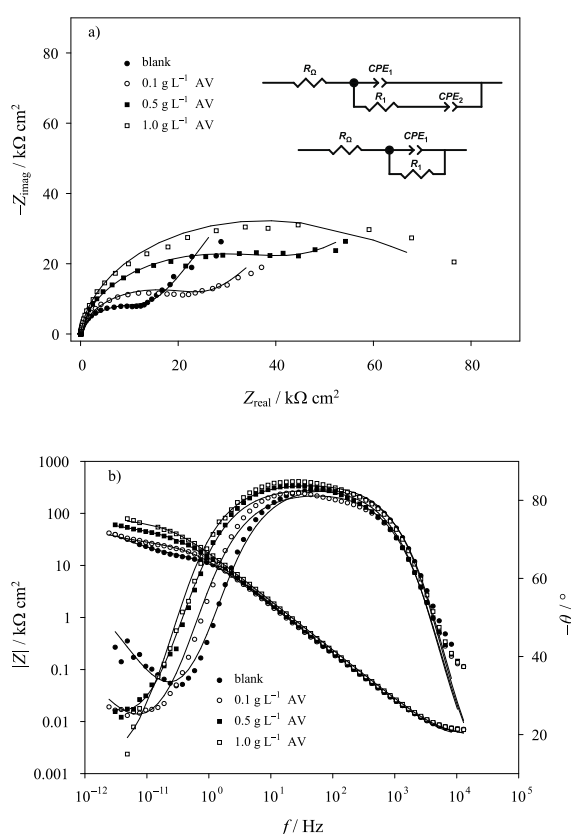


**Figure 4.** Impedance spectra (Nyquist and Bode plots) of the Al electrode recorded at the EOCp in 3 % NaCl solution, containing different concentrations of the AV extract (shown in figure).

with  $Q_1$  equal to the double-layer capacitance,  $C_{\text{dl}}$  and  $R_1$  represents the charge transfer resistance.<sup>[4,5]</sup> The second time constant is represented by CPE<sub>2</sub> with power  $n$  close to 0.5 that represents Warburg impedance which describes

the diffusion processes through the film (diffusion of oxygen or metal ions).<sup>[19,20]</sup> EEC used to describe impedance spectra of Al electrode in 3% NaCl with presence of 1.0 g L<sup>-1</sup> AV extract consists of a CPE<sub>1</sub> in the parallel to the resistor R<sub>1</sub>.

The Nyquist plots (Figure 4.a) show capacitive loop in the medium frequency region, which is associated with the thickness and dielectric properties of surface film. The increase of the semicircle radius with the increase of AV extract concentration indicates adsorption of AV extract on the surface of the aluminium.

From Bode plots (Figure 4.b) it can be seen that in the region of low frequency the presence of AV extract increases the impedance values and in the middle frequency range phase angle increases to -85° with the increase of AV extract concentration. This is due to the adsorption of AV extract on the surface of the aluminium.

Impedance parameters obtained from EIS measurements are given in Table 3. From Table 3. it can be seen that there is a decrease in Q<sub>1</sub> values (from 1.37 · 10<sup>-5</sup> to 1.00 · 10<sup>-5</sup> Ω<sup>-1</sup>s<sup>n</sup> cm<sup>-2</sup>) that can be explained by decrease in local dielectric constant surface layer and/or increase in the thickness of the electrical double layer due to the adsorbed layer of extract which protects further corrosion. Also, increase in charge transfer resistance (from 15 to 75 kΩ cm<sup>2</sup>) as the AV extract concentration increases shows significant surface coverage.<sup>[21,22]</sup> The surface coverage can be calculated from charge transfer resistance values according to the following equation:<sup>[5,23]</sup>

$$\theta = \frac{R_1 - R_1^0}{R_1} \quad (4)$$

where R<sub>1</sub><sup>0</sup> and R<sub>1</sub> are the charge transfer resistance of the Al in the absence and presence of AV extract. The values of the surface coverage and inhibition efficiency are presented in Table 3. and follow the same trend as the values determined from polarization measurements.

The presence of the AV extract on the Al electrode also decreases the diffusion processes through the film. For Al electrode in 3 % NaCl with addition of 1.0 g L<sup>-1</sup> AV diffusion is not recorded which means that the diffusion is reduced by adsorbed inhibitive layer of AV extract.

**Table 3.** Impedance parameters, surface coverage and inhibition efficiency for Al electrode in 3 % NaCl, with and without presence of AV extract.

$\gamma / \text{g L}^{-1}$	$Q_1 \times 10^5 / \Omega^{-1} \text{s}^n \text{cm}^{-2}$	$n_1$	$R / \text{k}\Omega \text{cm}^2$	$Q_2 \times 10^4 / \Omega^{-1} \text{s}^n \text{cm}^{-2}$	$n_2$	$\theta$	$\eta / \%$
blank	1.37	0.94	15.06	1.13	0.66	–	–
0.10	1.29	0.92	25.88	1.09	0.63	0.418	41.8
0.50	1.17	0.93	44.85	1.05	0.60	0.664	66.4
1.00	1.00	0.94	75.12	–	–	0.800	80.0

## Adsorption Mechanism

From the PP and EIS results, it is evidence that extracts of *Alchemilla vulgaris* L. adsorb on the active sites of aluminium and prevents aluminium dissolution in 3 % NaCl solution. The adsorption of extract molecules depends on the nature of extract molecules, nature and charge of metal and electrolyte properties.<sup>[24,25]</sup> To describe the adsorption behaviour adsorption isotherms were often used.

The degrees of surface coverage ( $\theta$ ) for different concentrations of AV extract were determined by potentiodynamic polarization and electrochemical impedance spectroscopy.

The obtained experimental data were tested graphically to fit different isotherms, to explain the relationship between the surface coverage  $\theta$  and the concentration of the adsorbed molecules.

The obtained linear plots of  $\log \theta$  against  $\log \gamma$  as shown in Figure 5. indicate that the experimental data could be described with the Freundlich adsorption isotherm that is given by the following equation:

$$\log \theta = \log K - n \log \gamma \quad (5)$$

where  $K$  is the equilibrium adsorption constant, and  $n$  ( $0 < n < 1$ ) is adsorption intensity.

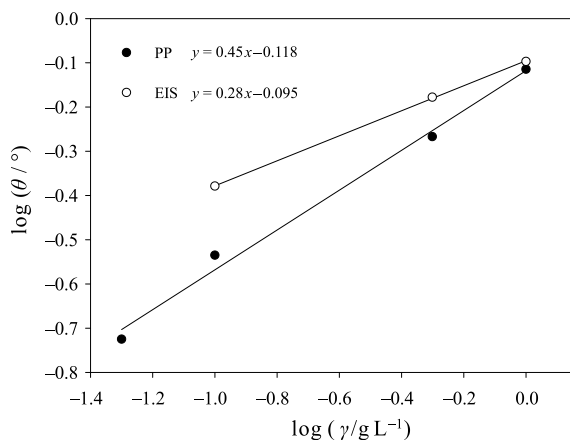


**Figure 5.** The Freundlich adsorption isotherm for the AV extract from PP and EIS measurements.

The equilibrium adsorption constant is related to the free energy of adsorption  $\Delta G^\circ$ :<sup>[5]</sup>

$$\Delta G^\circ = -RT \ln \left[ 1000 \left( \text{g L}^{-1} \right) \cdot K \left( \text{g}^{-1} \text{L} \right) \right] \quad (6)$$

where the value of 1000 is the mass concentration of water in the solution in  $\text{g L}^{-1}$ ,  $R$  is the universal gas constant and  $T$  is the absolute temperature. This multiplication was used to nullify the unit of  $K$  ( $\text{L g}^{-1}$ ) with 1000 g of water per L of aqueous solution.

The adsorption constant and the Gibbs energy were determined to be from PP data:  $K = 0.762$  and  $\Delta G = -16.44$   $\text{kJ mol}^{-1}$  and from EIS data:  $K = 0.804$  and  $\Delta G = -16.57$   $\text{kJ mol}^{-1}$ .

According to the literature, negative values of  $\Delta G$  below  $-20$   $\text{kJ mol}^{-1}$  are referred to physical adsorption which results from the Coloumbic interaction of the charged inhibitor molecules and the charged metal. The values of  $\Delta G$  above  $-40$   $\text{kJ mol}^{-1}$  are associated to chemisorptions by charge sharing or transfer from the inhibitor molecules to the metal surface to form a coordinate type of bond.<sup>[4,5,26]</sup> The calculated negative values of  $\Delta G$  confirm the spontaneous adsorption of AV extract on the Al surface by physisorption.

### Cyclic Voltammetry

The cyclic voltammograms of the aluminium recorded in 3% NaCl solution without and with presence of  $1.0$   $\text{g L}^{-1}$  AV extract are presented in Figure 6. The voltammogram of aluminium in pure 3% NaCl shows one anodic peak, A at around  $-1.0$  V that can be ascribed to the formation of a Al(III) oxide. The formation of oxide film on the Al surface is a typical irreversible process so in the cathodic scan reduction of anodically formed Al oxide is not recorded.<sup>[2,27,28]</sup>

The cyclic voltammogram of aluminium in 3% NaCl with addition of  $1.0$   $\text{g L}^{-1}$  AV extract shows two anodic peaks. First anodic peak,  $A_1$  is related to the accumulation of Al ions at the interface metal/solution (initial phase of oxide growth).<sup>[2,27]</sup> With the addition of  $1.0$   $\text{g L}^{-1}$  AV extract, current density in the potential range of peak A is decreased and the anodic peak A become less prominent. As the magnitude of the current density represents the reaction speed<sup>[19]</sup> it is clear that the dissolution rate of aluminium is lower in the presence of AV extract due to the adsorption of the organic molecules that block active sites on the Al surface.

**Table 4.** Anodic charges, film thickness, surface coverage and inhibition efficiency for the Al electrode in 3% NaCl with and without presence of  $1.0$   $\text{g L}^{-1}$  AV extract.

Solution $\gamma / \text{g L}^{-1}$	$Q_a / \text{mC cm}^{-2}$	$d / \text{nm}$	$\theta$	$\eta / \%$
blank	9.472	2.60	–	–
1.0	2.288	0.63	0.758	75.8

The total charges used for oxidation processes,  $Q_a$ , are determined by integration of the anodic part of cyclic voltammograms from Figure 4. (Table 4.). Values of anodic charges are used to calculate thicknesses,  $d$ , of the surface layers (Al(III) oxide) as follows:

$$d = \left( \frac{M}{\rho z F} \right) \frac{Q_a}{\sigma} \quad (7)$$

where  $M$  is the molar mass of  $\text{Al}_2\text{O}_3$ ,  $\rho$  is density of  $\text{Al}_2\text{O}_3$  ( $M/\rho = 31.80$   $\text{cm}^3 \text{mol}^{-1}$ ),  $z$  is the number of electrons,  $F$  is the Faraday constant and  $\sigma$  is the roughness factor of the surface ( $\sigma = 2$ ).

Determined anodic charges are used to calculate the surface coverage,  $\theta$  according to the equation:

$$\theta = \frac{Q_A^0 - Q_A}{Q_A^0} \quad (8)$$

A where  $Q_A^0$  and  $Q_A$  represent anodic charges in the absence and presence of the extract. Inhibition efficiency,  $\eta$  is calculated according to the equation (2) and presented in Table 4. together with anodic charges, film thickness and surface coverage value.

The value of inhibition efficiency for Al electrode in 3% NaCl with addition of  $1.0$   $\text{g L}^{-1}$  AV (75.8%) is in good agreement with the values determined from the polarization measurements and impedance spectroscopy.

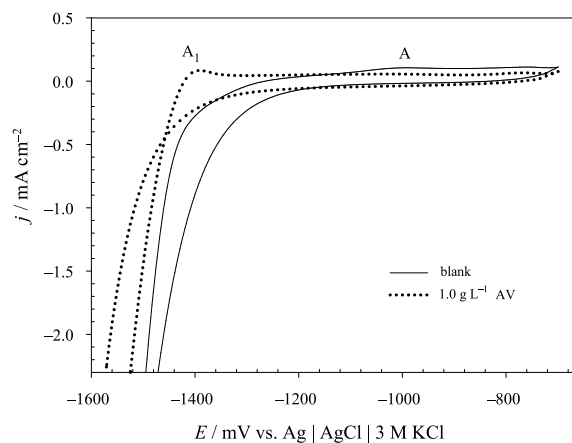


**Figure 6.** Cyclic voltammograms for the Al electrode 3% NaCl solution without and with  $1.0$   $\text{g L}^{-1}$  AV extract (shown in figure);  $\nu = 30$   $\text{mV s}^{-1}$ .

## CONCLUSIONS

In this work, *Alchemilla vulgaris* L. extract (AV) was successfully tested as an eco-friendly corrosion inhibitor for aluminium in 3 % NaCl using electrochemical techniques. Polarization measurements showed that AV extract works as a mixed-type inhibitor. By raising the concentration of AV extract, the inhibition efficiency increases due to its adsorption on the Al surface with maximal efficiency around 80 % at 1.0 g L<sup>-1</sup>. Adsorption of the extract molecules obeys Freundlich isotherm, with physisorption mechanism ( $\Delta G \approx -16$  kJ mol<sup>-1</sup>). The activation energy increases with the addition of AV extract (from 52.7 kJ mol<sup>-1</sup> to 89.2 kJ mol<sup>-1</sup>) indicating adsorption of extract molecules on Al surface. The impedance results showed that with the addition of AV extract resistance values increase (from 15 to 75 k $\Omega$  cm<sup>2</sup>) and diffusion process through the surface layer is suppressed. Cyclic voltammetry results also reveal that aluminium dissolution is more pronounced in the absence of AV extract. All experimental results were consistent with each other and showed that AV extract forms a layer on the Al surface and prevents the dissolution of aluminium in 3 % NaCl.

## REFERENCES

- [1] S. C. Udensi, O. E. Ekpe, L. A. Nnanna, *Sci. Afr.* **2021**, *12*, e00791. <https://doi.org/10.1016/j.sciaf.2021.e00791>
- [2] Z. Pilić, I. Martinović, *Int. J. Electrochem. Sci.* **2017**, *12*, 3576–3588. <https://doi.org/10.20964/2017.05.46>
- [3] N. Raghavendra, *Chemistry Africa* **2020**, *3*, 21–34. <https://doi.org/10.1007/s42250-019-00114-6>
- [4] Z. Pilić, I. Martinović, *Chem. Biochem. Eng. Q.* **2019**, *33*, 449–457. <https://doi.org/10.15255/CABEQ.2019.1614>
- [5] Z. Pilić, I. Martinović, M. Pavlinović, G. Zlatić, *Croat. Chem. Acta* **2019**, *92*, 79–85. <https://doi.org/10.5562/cca3451>
- [6] R. S. Nathiya, S. Perumal, V. Murugesan, V. Raj, *Mater Sci Semicond Process* **2019**, *104*, 104674. <https://doi.org/10.1016/j.mssp.2019.104674>
- [7] H. Elgahawi, M. Gobara, A. Baraka, W. Elthalabawy, *J. Bio-Tribo-Corros.* **2017**, *3*, 55. <https://doi.org/10.1007/s40735-017-0116-x>
- [8] A. S. Fouda, H. S. Gadow, E. G. Abd Elal, M. I. El-Tantawy, *J. Bio-Tribo-Corros.* **2021**, *7*, 102. <https://doi.org/10.1007/s40735-021-00527-2>
- [9] M. Prabakaran, S.-H. Kim, A. Sasireka, K. Kalaiselvi, I.-M. Chung, *J Adhes Sci Technol* **2018**, *32*, 2054–2069. <https://doi.org/10.1080/01694243.2018.1462947>
- [10] S. Vlajsavljević, S. Jelača, G. Zengin, N. Mimica-Dukić, S. Berežni, M. Miljić, Z. D. Stevanović, *RSC Adv.* **2019**, *9*, 37474–37483. <https://doi.org/10.1039/C9RA08231J>
- [11] R. K. Ahmed, S. Zhang, *Int. J. Electrochem. Sci.* **2019**, *14*, 10657–10669. <https://doi.org/10.20964/2019.11.43>
- [12] R. Salghi, S. Jodeh, E. E. Ebenso, H. Lgaz, D. B. Hmamou, M. Belkhaouda, T. H. Ali, M. Messali, B. Hammouti, S. Fattouch, *Int. J. Electrochem. Sci.* **2017**, *12*, 3283–3295. <https://doi.org/10.20964/2017.04.46>
- [13] A. M. Eldesoky, M.A. Diab, A. Z. El-Sonbati, S.F. Salam, *Int. J. Electrochem. Sci.* **2017**, *12*, 4215–4237.
- [14] L. K. S. Hassane, I. Saha, C. Abdelkarim, B. K. Subrahmanya, S. Rachid D. Shubhalaxmi, B. Priyabrata, H. A. Ismat, I. Mohammad, F. Khan, C. Min, *Constr. Build Mater.* **2020**, *233*, 117320. <https://doi.org/10.1016/j.conbuildmat.2019.117320>
- [15] E. Baran, A. Cakir, B. Yazici, *Arab. J. Chem.* *Arabian Journal of Chemistry* **2019**, *12*, 4303–4319. <https://doi.org/10.1016/j.arabjc.2016.06.008>
- [16] X. L. Zhanga, Z. H. Jiang, Z. P. Yao, Y. Song, Z. D. Wu, *Corr. Sci.* **2009**, *15*, 581–587. <https://doi.org/10.1016/j.corsci.2008.12.005>
- [17] L. Xianghong, D. Shuduan, F. Hui, X. Xiaoguang, *Corr. Sci.* **2014**, *78*, 29.
- [18] H. Bourazmi, M. Tabyaoui, L. EL-Hattabi, Y. El-Aoufr, E. E. Ebenso, A. Ansari, *J. Mater. Environ. Sci* **2018**, *9*, 1058–1074. <https://doi.org/10.26872/jmes.2017.9.3.118>
- [19] Z. Liang, K. Jiang, T. Zhang, Z. Dou, *Mater. Corros.* **2019**, *71*, 4, 617–627. <https://doi.org/10.1002/maco.201911338>
- [20] Y. Chen, D. M. Qi, H. P. Wang, Z. Xu, C. X. Yi, Z. Zhang, *Int. J. Electrochem. Sci.* **2015**, *10*, 9056–9072.
- [21] S. Murlidharan, K. L. N. Phani, S. Pitchumani, S. Ravichandran, *J. Electrochem. Soc.* **1995**, *142*, 1478–1483. <https://doi.org/10.1149/1.2048599>
- [22] F. Bentiss, M. Traisnel, M. Lagrenee, *Corros. Sci.* **2000**, *42*, 127–146. [https://doi.org/10.1016/S0010-938X\(99\)00049-9](https://doi.org/10.1016/S0010-938X(99)00049-9)
- [23] S. Shen, X. Guo, P. Song, Y.-C. Pan, H. Wang, Y. Wen, H.-F. Yang, *Appl. Surf. Sci.* **2013**, *276*, 167–173. <https://doi.org/10.1016/j.apsusc.2013.03.061>
- [24] O. Benali, M. Ouazene, *Arab. J. Chem.* **2011**, *4*, 443–448. <https://doi.org/10.1016/j.arabjc.2010.07.016>
- [25] A. Anejjar, R. Salghi, A. Zarrouk, O. Benali, H. Zarrok, B. Hammouti, S. S. AlDeyab, N. Benchat, A. Elaattiaoui, *J. Electrochem. Sci.* **2013**, *8*, 11512–11525.
- [26] V. Grudić, I. Bošković, A. Gezović, *Chem. Biochem. Eng. Q.* **2018**, *32*, 299–305. <https://doi.org/10.15255/CABEQ.2018.1357>
- [27] D. Hasenay, M. Šeruga, *J. Appl. Electrochem.* **2007**, *37*, 1001–1008. <https://doi.org/10.1007/s10800-007-9339-8>
- [28] S. Gudić, J. Radošević, D. Krpan-Lisica, M. Kliškić, *Electrochim. Acta*, **2001**, *46*, 2515–2526. [https://doi.org/10.1016/S0013-4686\(01\)00473-X](https://doi.org/10.1016/S0013-4686(01)00473-X)